frontiers in Astronomy and Space Sciences

ORIGINAL RESEARCH
published: 20 April 2021
doi: 10.3389/fspas.2021.668587

The NUMEN Project: An Update of the Facility Toward the Future Experimental Campaigns

Francesco Cappuzzello[1,2], Luis Acosta[3], Clementina Agodi[2], Ismail Boztosun[4], Giuseppe A. Brischetto[1,2], Salvatore Calabrese[2], Luciano Calabretta[2], Daniela Calvo[5], Luigi Campajola[6,7], Vittoria Capirossi[5,8], Diana Carbone[2], Manuela Cavallaro[2], Efrain Chávez[3], Irene Ciraldo[1,2], Franck Delaunay[1,2,9], Haris Djapo[10], Carlo Ferraresi[5,11], Paolo Finocchiaro[2], Maria Fisichella[2], Elisa M. Gandolfo[6,7], Felice Iazzi[5,8], Mauricio Moralles[12], Lorenzo Neri[2], Josè R. B. Oliveira[13], Luciano Pandola[2], Horia Petrascu[14], Federico Pinna[5,8], Antonio D. Russo[2], Diego Sartirana[5], Onoufrios Sgouros[2], S. O. Solakci[4], Vasileios Soukeras[2], Alessandro Spatafora[1,2], Domenico Torresi[2], Salvatore Tudisco[2] and Aydin Yildirim[4] on behalf of the NUMEN collaboration*

[1] Dipartimento di Fisica e Astronomia "Ettore Majorana", Università di Catania, Catania, Italy, [2] Istituto Nazionale di Fisica Nucleare–Laboratori Nazionali del Sud, Catania, Italy, [3] Instituto de Física, Universidad Nacional Autónoma de México, Mexico City, Mexico, [4] Physics Department, Akdeniz University, Antalya, Turkey, [5] Istituto Nazionale di Fisica Nucleare–Sezione di Torino, Turin, Italy, [6] Dipartimento di Fisica–Università di Napoli Federico II, Napoli, Italy, [7] Istituto Nazionale di Fisica Nucleare–Sezione Napoli, Napoli, Italy, [8] Dipartimento Scienza Applicata e Tecnologia, Politecnico di Torino, Torino, Italy, [9] LPC Caen, Normandie Université, ENSICAEN, UNICAEN, CNRS/IN2P3, Caen, France, [10] Institute of Accelerator Laboratory, Ankara University, Ankara, Turkey, [11] Dipartimento di Ingegneria Meccanica e Aerospaziale, Politecnico di Torino, Turin, Italy, [12] Instituto de Pesquisas Energéticas e Nucleares, Instituto de Pesquisas Energéticas e Nucleares, Comissão Nacional de Energia Nuclear, São Paulo, Brazil, [13] Instituto de Física da Universidade de São Paulo, São Paulo, Brazil, [14] Institutul National de Cercetare-Dezvoltare pentru Fizica si Inginerie Nucleara Horia Hulubei (IFIN-HH), Măgurele, Romania

The goal of NUMEN project is to access experimentally driven information on Nuclear Matrix Elements (NME) involved in the neutrinoless double beta decay ($0\nu\beta\beta$) by accurate measurements of the cross sections of heavy-ion induced double charge-exchange reactions. In particular, the (^{18}O, ^{18}Ne) and (^{20}Ne, ^{20}O) reactions are adopted as tools for $\beta^+\beta^+$ and $\beta^-\beta^-$ decays, respectively. The experiments are performed at INFN–Laboratory Nazionali del Sud (LNS) in Catania using the Superconducting Cyclotron to accelerate the beams and the MAGNEX magnetic spectrometer to detect the reaction products. The measured cross sections are very low, limiting the present exploration to few selected isotopes of interest in the context of typically low-yield experimental runs. In order to make feasible a systematic study of all the candidate nuclei, a major upgrade of the LNS facility is foreseen to increase the experimental yield by more than two orders of magnitude. To this purpose, frontier technologies are being developed for both the accelerator and the detection systems. An update description of the NUMEN project is presented here, focusing on recent achievements from the R&D activity.

Keywords: double beta decay, nuclear matrix elements, double charge exchange, heavy ion multidetector, MAGNEX spectrometer

OPEN ACCESS

Edited by:
Giuseppe Mandaglio, University of Messina, Italy

Reviewed by:
Michał Silarski, Jagiellonian University, Poland
Andrea Celentano, Universities and Research, Italy

****Correspondence:***
Francesco Cappuzzello
cappuzzello@lns.infn.it

Specialty section:
This article was submitted to Nuclear Physics, a section of the journal Frontiers in Astronomy and Space Sciences

Received: *16 February 2021*
Accepted: *18 March 2021*
Published: *20 April 2021*

Citation:
Cappuzzello F, Acosta L, Agodi C, Boztosun I, Brischetto GA, Calabrese S, Calabretta L, Calvo D, Campajola L, Capirossi V, Carbone D, Cavallaro M, Chávez E, Ciraldo I, Delaunay F, Djapo H, Ferraresi C, Finocchiaro P, Fisichella M, Gandolfo EM, Iazzi F, Moralles M, Neri L, Oliveira JRB, Pandola L, Petrascu H, Pinna F, Russo AD, Sartirana D, Sgouros O, Solakci SO, Soukeras V, Spatafora A, Torresi D, Tudisco S and Yildirim A (2021) The NUMEN Project: An Update of the Facility Toward the Future Experimental Campaigns. Front. Astron. Space Sci. 8:668587. doi: 10.3389/fspas.2021.668587

INTRODUCTION

Neutrinoless double beta decay ($0\nu\beta\beta$) is a nuclear process where a parent nucleus decays into a daughter isobar differing by two units of charge and two electrons (or positrons) are emitted. Although not yet observed, this phenomenon is nowadays widely investigated since, if discovered in the experiments, it would allow to directly determine the Majorana nature of neutrino and unveil that the total lepton number is not necessarily conserved in nature (Suhonen and Civitarese, 2012; Vergados et al., 2012; Gouvea and Vogel, 2013). Moreover, the neutrino effective mass could be extracted from decay rate measurements, with foreseen sensitivity to normal or inverted hierarchy scenarios in the neutrino mass distribution. Presently, this physics case is leading the research "beyond the standard model" as it could help to explain the matter–antimatter asymmetry observed in the Universe and open new perspectives toward a grand unified theory of fundamental interactions.

Double beta decay occurs in atomic nuclei, making nuclear structure issues essential for its proper description. The $0\nu\beta\beta$ decay rate is typically expressed as the product of three main factors: (i) a phase-space parameter, describing the motion of the electrons (or positrons); (ii) the square of a nuclear matrix element (NME), connected to the overlap between the initial and final nuclear states; (iii) a factor describing the emission and reabsorption of the neutrino, containing physics beyond the standard model. Thus, if the NMEs are established with sufficient precision, new physics can be accessed from $0\nu\beta\beta$ decay rate measurements.

A deeper knowledge of the NMEs is thus crucial to set the strategies of future experiments of direct search for $0\nu\beta\beta$ decay. However, an updated comparison of the results of NMEs calculations, obtained within various nuclear structure frameworks (Barea et al., 2013; Dell'Oro et al., 2016; Ejiri et al., 2019), indicates that significant differences (about a factor three) are indeed found, which makes the present situation not satisfactory. To date the determination of the NMEs, based on different calculation schemes, is still controversial, also due to the lack of experimental constraints.

Over the last few years, major interest has raised for heavy-ion induced Double Charge-Exchange (DCE) studies, especially because of their possible connection to $0\nu\beta\beta$ decay. Exploratory studies have been started at RIKEN in Tokyo and at RCNP in Osaka (Matsubara et al., 2013; Kisamori et al., 2016; Takahisa et al., 2017). An intense activity is also being pursued at the Istituto Nazionale di Fisica Nucleare–Laboratori Nazionali del Sud (INFN-LNS) in Catania, in the frame of the NUMEN project. A new DCE reaction, the (^{20}Ne,^{20}O), has been recently studied for the first time, looking for $\beta^-\beta^-$-like transitions. In addition, important results have been achieved on the $\beta^+\beta^+$ side by the renewed use of the (^{18}O,^{18}Ne) reaction in upgraded experimental conditions. NUMEN and the synergic NURE (ERC Starting Grant 2016) project at INFN-LNS (Agodi et al., 2015; Cappuzzello et al., 2015a, 2018; Cavallaro et al., 2017; Cappuzzello and Agodi, 2021) aim at extracting nuclear structure information relevant for $0\nu\beta\beta$ NMEs by measuring cross sections of DCE and Single Charge Exchange (SCE) reactions. Recent theoretical developments suggest that besides the transition to the ground state of the residual nucleus, the whole double Gamow-Teller strength could, in principle, be connected to $0\nu\beta\beta$-NME (Sagawa and Uesaka, 2016; Santopinto et al., 2018; Shimizu et al., 2018). In particular, results from state-of-art shell-model calculations indicate that a simple relation is expected between the $0\nu\beta\beta$ NME for ^{48}Ca and the centroid energy of the still not observed double Gamow-Teller giant resonance (DGTGR) (Shimizu et al., 2018). In addition, an interesting linear correlation is found between the DGT transition to the ground state of the final nucleus and the $0\nu\beta\beta$ decay NME, even adopting other nuclear structure models.

Since the DGTGR is expected to almost exhaust the corresponding model independent sum rule (Sagawa and Uesaka, 2016), the experimental determination of its strength will also give quantitative access to the quenching of the nuclear response to second order spin-isospin operators. This is particularly interesting because of its connection to long debated problem of the quenching of the axial coupling constant in $0\nu\beta\beta$ decay (Suhonen, 2017). A renormalization of the coupling constant (quenching) of second order spin-isospin (GT-like) operators is indeed expected, due to limitations of the model spaces adopted in the NME calculations and to the typical neglect of two-body currents (Engel and Menendez, 2017; Cappuzzello and Cavallaro, 2020). The exact value of this quenching is still controversial despite it enters to the fourth power in the determination of the $0\nu\beta\beta$ decay rates and could drastically impact on the sensitivity of different experiments searching for that. No experimental evidence of the DGTGR has been reported until now, which makes the possible discovery of this mode a ground-breaking result by itself. Thus, it is not surprising that NUMEN as well as the projects at RIKEN are also targeting the DGTGR resonance.

The aim of the NUMEN project is to measure the absolute cross section for heavy-ion induced DCE reactions on nuclei candidates for the $0\nu\beta\beta$ decay and find a connection between the NMEs of the two processes. Even if $0\nu\beta\beta$ decays and DCE reactions are mediated by different interactions, there are a number of similarities among them: the key aspects are that initial and final nuclear states are the same and the transition operators in both cases are a superposition of short-range isospin, spin-isospin and rank-two tensor components with a relevant available momentum (100 MeV/c or so). The strong interaction mediating the HIDCE makes these processes much more likely to occur compared to $0\nu\beta\beta$ decay. In this way the many body nuclear states involved in the $0\nu\beta\beta$ decay can be explored under controlled laboratory conditions.

In DCE reactions the nuclear matrix elements enter in the expression of the cross section, which is the observable deserving the main interest. However, the DCE reaction channel competes with other nuclear processes activated by the projectile-target collision, many of which are much more likely to occur. As a consequence, the experimental challenge is to isolate and measure a very rare nuclear transition among a very high rate of reaction products generated by the beam-target interaction. In Cappuzzello et al. (2015b) the ^{40}Ca(^{18}O,^{18}Ne)^{40}Ar reaction was studied at 15 MeV/u at the MAGNEX facility of INFN-LNS laboratory (Cappuzzello et al., 2016), showing that

high mass, angular and energy resolution energy spectra and accurate absolute cross sections can be measured, even at very forward scattering angles. With respect to this pilot experiment, additional difficulties are foreseen for the exploration of DCE on nuclei of interest for 0νββ research. As discussed in Cappuzzello et al. (2018), the present limits of the facility in terms of beam power for the Superconducting Cyclotron accelerator and the acceptable rate of few kHz for the MAGNEX focal plane detector (FPD) have limited so far the exploration of DCE to only few cases (e.g., ^{12}C, ^{40}Ca,^{48}Ti, ^{76}Ge, ^{76}Se, ^{116}Cd, ^{116}Sn, ^{130}Te) with beam power of few W. The systematic exploration of all the nuclei of interest for 0νββ decay, foreseen in the NUMEN project, needs an upgraded set-up able to work with kW beam power (Agodi et al., 2021).

NUMEN is also fostering the development of a specific theory program to allow an accurate extraction of nuclear structure information from the measured cross sections. Heavy ion induced SCE reactions have been analyzed in detail in Cappuzzello et al. (2004), Lenske et al. (2018), Lenske et al. (2019) in view of the connection to single beta decay NME. It was shown that the surface localization of the SCE, due the strong absorption of the target-projectile nucleus-nucleus potential, allows for a decisive simplification of the reaction description, making the isovector meson exchange mechanism dominant at forward detection angles. The development of a second order perturbation scheme for DCE cross section is being accomplished relying on quantum mechanical scattering theory, within the Distorted Wave Born Approximation. The theory is focused on the development of microscopic models for DCE reactions, employing several approaches (QRPA, shell model, IBM) for inputs connected to nuclear structure quantities. The link between the theoretical description of the 0νββ decay and DCE reactions is also under study (Santopinto et al., 2018; Lenske et al., 2019; Bellone et al., 2020; Magana Vsevolodovna et al., 2021).

Part of the plans and activities in view of the upgrade of the experimental facility is described in Cappuzzello et al. (2018), Finocchiaro et al. (2020), Agodi et al. (2021), while recent experimental results from NUMEN are cited in Section Experimental activity with accelerated beams during numen phase 2. In this manuscript an update of the NUMEN R&D activity is given, with special emphasis on recent advances on technical aspects not presented elsewhere.

EXPERIMENTAL ACTIVITY WITH ACCELERATED BEAMS DURING NUMEN PHASE 2

Experimental Setup

The NUMEN experiments have been performed at INFN-LNS, using the available high performing experimental facilities, mainly constituted by the K800 superconducting cyclotron (CS) and the MAGNEX magnetic spectrometer.

The CS accelerates the required ion beams, namely ^{18}O, ^{20}Ne, at energies ranging from 15 to 30 MeV/u with high energy resolution (1/1,000) (Cappuzzello et al., 2014) and low emittance (∼2π mm mr) (Rifuggiato et al., 2013). So far, the maximum cyclotron beam power could not exceed ∼100 W, which has not been an issue for the NUMEN Phase 2 experiments, due to more stringent limitations from the present detectors installed at the MAGNEX focal plane. Both facilities need to be upgraded in view of the future experimental campaign (NUMEN Phase 4), where beam power of few kW on target are demanded. An overview of the ongoing upgrade of the CS is found in Agodi et al. (2021).

The MAGNEX spectrometer is a large acceptance magnetic device consisting of a large aperture vertically focusing quadrupole and a horizontally bending dipole magnet (Cappuzzello et al., 2016). A picture of the MAGNEX spectrometer is shown in **Figure 1**. MAGNEX was designed to investigate heavy-ion induced reactions down to very low cross sections allowing the identification of the reaction products with good mass ($\Delta A/A \sim 1/160$), angle ($\Delta\theta \sim 0.2^{\circ}$), and energy resolution ($\Delta E/E \sim 1/1{,}000$), within a large solid angle ($\Omega \sim 50$ msr) and momentum range ($-14\% < \Delta p/p < +10\%$). High-resolution measurements for quasi-elastic processes, characterized by differential cross sections falling down to tens of nb/sr, were already performed with this setup (Pereira et al., 2012; Oliveira et al., 2013; Cappuzzello et al., 2015b,c; Calabrese et al., 2018) even at very forward scattering angles. A crucial feature is the implementation of the powerful technique of trajectory reconstruction, based on differential algebra, which solves the equation of motion of each detected particle up to 10th order (Cappuzzello et al., 2011). This is a unique characteristic of MAGNEX, which guarantees the above-mentioned performances and its relevance in the worldwide scenario of heavy-ion physics also taking advantage of its coupling to the EDEN neutron detector array (Cavallaro et al., 2016).

The MAGNEX FPD consists of a large (active volume 1,360 × 200 × 96 mm) low-pressure gas-filled tracker followed by a wall of 60 silicon pad sensors stopping the detected ions (Cavallaro et al., 2012; Torresi et al., 2021). A set of wire-based drift chambers measures the vertical position and angle of the reaction ejectiles, while the horizontal position and angle are extracted from the induced charge distributions on a set of segmented pads (Carbone et al., 2012). The energy loss measured by the multiplication wires and the residual energy at the silicon

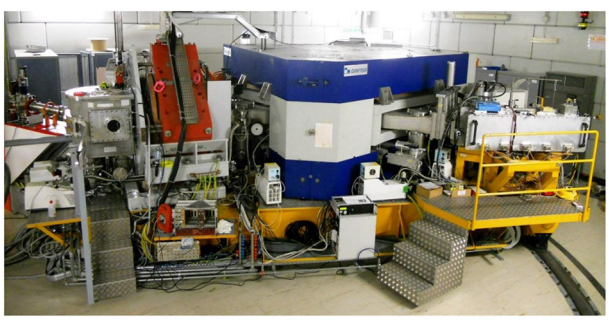

FIGURE 1 | View of the MAGNEX spectrometer at INFN-LNS.

TABLE 1 | List of the reactions explored during NUMEN Phase 2 together with references.

Projectile-Ejectile system	Reaction channel	References
(^{18}O,^{18}O)	Elastic and inelastic scattering	Carbone et al., 2021; Cavallaro et al., 2021; La Fauci et al., 2021
(^{18}O,^{18}Ne)	DCE reaction	Cappuzzello et al., 2015b
(^{18}O,^{18}F)	SCE reaction	Cavallaro et al., 2021
(^{18}O,^{17}O)	One-Neutron stripping reaction	(Ciraldo et al., in preparation)
(^{18}O,^{16}O)	Two-Neutron stripping reaction	Cappuzzello et al., 2021
(^{18}O,^{19}F)	One-Proton pickup reaction	(Ciraldo and Nuovo Cimento, submitted)
(^{18}O,^{20}Ne)	Two-Proton pickup reaction	Ferreira et al., 2021
(^{20}Ne,^{20}Ne)	Elastic and inelastic scattering	Spatafora et al., 2019; Carbone et al., 2021
(^{20}Ne,^{20}O)	DCE reaction	Calabrese et al., 2018, 2020
(^{20}Ne,^{20}F)	SCE reaction	(Burrello et al., in preparation)
(^{20}Ne,^{21}Ne)	One-Neutron pickup reaction	–
(^{20}Ne,^{22}Ne)	Two-Neutron pickup reaction	Carbone et al., 2020
(^{20}Ne,^{19}F)	One-Proton stripping reaction	(Burrello et al., in preparation)
(^{20}Ne,^{18}O)	Two-Proton stripping reaction	Carbone et al., 2020

detectors are used for atomic number (Z) identification of the ions. The ratio m/q between the ion mass (m) and charge (q) is determined by correlating the measured energy and impact position in the spectrometer horizontal (dispersive) direction, as described in Cappuzzello et al. (2010). The present FPD is a suitable detector to discriminate ions with 0.6% resolution in m/q and 2% in Z. The tracking measurement sensitivity guarantees an overall energy resolution of about 1/1,000, which is close to the limit of the optics for the used beams. The performances of the present FPD are described in Torresi et al. (2021).

Experimental Activity

The Phase 2 of NUMEN has been recently concluded with the last experiment performed at INFN LNS in June 2020 before the shutdown of the accelerator machines needed for the planned facility upgrade (Agodi et al., 2021).

The Phase 2 in-beam experimental activity targeted two classes of measurements, characterized by the acceleration of CS beams and the detection of specific reaction ejectiles with the MAGNEX spectrometer. The two classes correspond to the exploration of the two directions of isospin lowering and raising operators, characteristic of $\beta^-\beta^-$ and $\beta^+\beta^+$ decay, respectively. In particular, the investigation of the isospin raising transitions in the target has been performed using ^{18}O beams and studying the (^{18}O,^{18}Ne) double charge exchange transitions in the projectile, while the isospin lowering direction in the target has been explored using ^{20}Ne beams via the (^{20}Ne,^{20}O) DCE reaction (Cavallaro et al., 2020). For both classes of experiments, besides the DCE reaction channel, other scattering and reactions channels characterized by the same projectile and target at the same dynamical conditions have been studied. **Table 1** lists the reactions investigated in NUMEN Phase 2, together with the already available references to publication. **Figure 2** gives a comprehensive schematic representation of the already explored reactions, where also the involved target and residual nuclei are indicated.

A limited number of isotopes were selected as target systems in the Phase 2 experiments as result of a compromise between the interest of the scientific community to specific ββ emitter candidates and technical issues. These latter are also connected with the complex target production technologies and the expected energy resolution necessary to isolate the ground-to ground state transition in the DCE measured energy spectra.

The target isotopes explored via the (^{18}O,^{18}Ne) reaction at 15 MeV/u are ^{48}Ti, ^{76}Se, ^{116}Sn with the aim of studying the ^{48}Ti $\rightarrow$ ^{48}Ca, ^{76}Se $\rightarrow$ ^{76}Ge and ^{116}Sn $\rightarrow$ ^{116}Cd DCE transitions, respectively, together with the competing channels listed in **Table 1**. The ^{40}Ca $\rightarrow$ ^{40}Ar and ^{12}C $\rightarrow$ ^{12}Be transitions were also studied as test cases for the experimental and theoretical analyses at two different energies, 15 and 22 MeV/u. The measurements at very forward angles, including zero degree, were performed by placing the spectrometer optical axis at $+3^\circ$ with respect to the incident beam axis. Thanks to its large angular acceptance, the $-2^\circ < \theta_{lab} < +9^\circ$ range was explored. A specifically designed Faraday cup, located in a region aside the FPD, stopped the beam and measured the incident charge in each run for the determination of the absolute cross section.

The target isotopes explored by the (^{20}Ne,^{20}O) DCE reaction at 15 MeV/u are ^{116}Cd (to study the ^{116}Cd $\rightarrow$ ^{116}Sn transition), ^{130}Te (for ^{130}Te $\rightarrow$ ^{130}Xe) and ^{76}Ge (for ^{76}Ge $\rightarrow$ ^{76}Se). For these experiments, the spectrometer optical axis was typically placed at -3°, covering an angular range $-8^\circ < \theta_{lab} < +3^\circ$. A different Faraday cup, located in the high-magnetic-rigidity region aside the FPD was used in these experiments, as described in Cavallaro et al. (2020).

RECENT TECHNICAL ACHIEVEMENTS

Several recent accomplishments have been achieved by NUMEN, while it is moving from the intense experimental and R&D activity of Phase 2 toward the construction of the new upgraded elements. The evolution of the different aspects of the project, by means of laboratory tests on prototypes, simulations and the development of technical drawings is allowing for the continuous fine tuning of all the elements under study. In this section some of the most relevant new results are briefly presented.

Target Characterization

The NUMEN target system must face two main requirements: the first is related to the heat dissipation, the second is related to the energy resolution constraints (Cappuzzello et al., 2018).

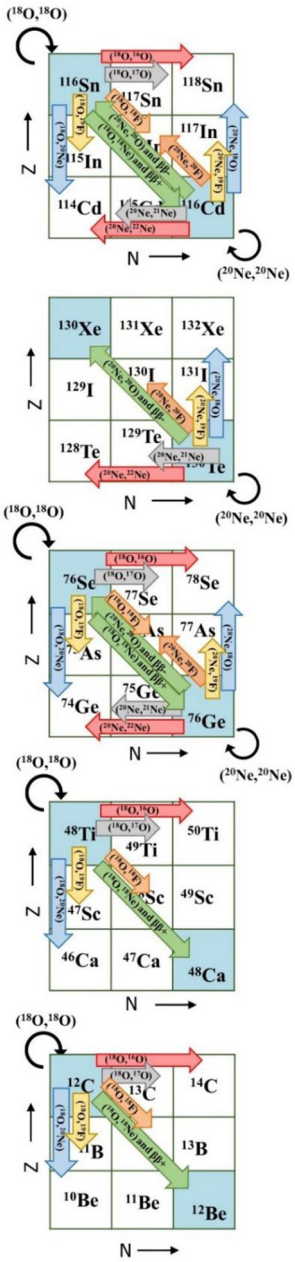

FIGURE 2 | Diagram of the reactions explored by the NUMEN project so far. The labels inside the arrows indicate the projectile-ejectile systems for each nuclear reaction channel, while the nuclei indicated in the squares are the target and residual systems populated by the reaction of the corresponding arrow.

The necessity of quickly dissipating the heat generated by the intense ion beam (up to 10^{13} pps) in the target led to a composite design of the target system. The isotopic material, required to build the target for DCE reactions, will be deposited on a substrate of Highly Oriented Pyrolytic Graphite (HOPG) (Iazzi et al., 2017; Pinna et al., 2020a). This type of graphite has a very high in-plane thermal conductivity, making this substrate

TABLE 2 | Target parameters extracted from RBS and APT measurements. See text.

Sample	$\bar{x}_{APT}$[nm]	*R* (APT) %	$\bar{x}_{RBS}$[nm]	Δ%
A25 (Ge)	530	6	535	1
B22 (Ge)	405	16	385	5
C11 (Ge)	350	6	535	1
A14 (Te)	430	6	425	1
B10 (Te)	435	11	415	4
C4 (Te)	435	1	420	4
A20 (Sn)	235	44	250	6
B4 (Sn)	230	68	260	12
C7 (Sn)	170	62	160	7

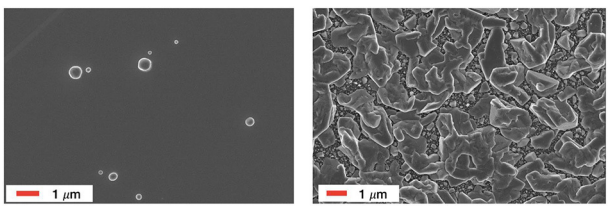

FIGURE 3 | FESEM images of the B22 (∼400 nm natural Germanium evaporated on 5 μm HOPG backing) (left) and B4 (∼250 nm natural Tin evaporated on 5 μm HOPG backing) (right) target samples.

able to quickly transfer the heat from the target center, hit by the ion beam, to the target extremities in contact with a cooled frame.

The energy resolution requirements of the NUMEN experiments limit the target thickness. Due to the interaction of the incident ions and the ejectiles produced by the nuclear reactions with the target material, energy dispersion and straggling occur proportionally to the target thickness. For this reason, the targets, including possible substrates, should be made as thin and uniform as possible. In addition, as discussed in Lo Presti et al. (2020) and in Section Radiation level, the amount of target material impacts on the overall radiation level in the MAGNEX experimental hall, during beam time operations and on the remnant activation afterward. Thus, a thinner target would be helpful also to mitigate this drawback. However, the reduction of the target thickness directly suppresses the yield collected in the experiments, which is a relevant issue especially for suppressed reaction channels such as DCE. A search for the optimal compromise depends on several aspects also connected to the chemical and thermodynamical properties of the involved materials. An extensive investigation of the problem leads us to target thickness in the range 250–450 nm for almost all the isotopes of interest and a few micrometers for the HOPG substrate.

The determination of the thickness of target and substrate is of crucial importance, as well as the knowledge of their thickness uniformity: the target system characterization is thus very important and has been subject of R&D study (Capirossi et al., 2020). In order to get as much information

as possible on the target samples and characterize the NUMEN target system, several analysis techniques have been adopted. In particular, Rutherford Backscattering Spectroscopy (RBS) and Alpha Particle Transmission (APT) techniques have been exploited to measure the thickness and the uniformity of target layer and substrate.

Both the techniques can provide precise evaluations of the average thickness of the sample, but only with APT the thickness uniformity can be quantified. The thickness obtained by APT can be verified with the RBS, while the quality of the isotopic layer deposition can be evaluated by studying the sample surface by Field Emission Scanning Electron Microscopy, which provides images of the sample surface topography.

The target thickness measurements with RBS and APT are listed in **Table 2**, together with the uniformity parameter R, defined as $R = \frac{\sigma_{nu}}{\overline{x}}$, where σ_{nu} is the standard deviation and $\overline{x}$ is the average value of the peak in the thickness distribution. The first column shows the labels of the target system prototypes. The first three rows are related to natural Germanium targets, the following three to natural Tellurium and the last three to natural Tin. The targets with labels beginning with the letter A, B and C have a HOPG substrate 10 μm, 5 μm and 2 μm thick, respectively. The fifth column indicates the parameter, calculated as the ratio $\Delta = \frac{\delta}{x}$, where δ is the difference and x is the average between the thickness measured by APT and RBS.

Table 2 shows that the agreement on the thickness evaluation between APT and RBS techniques is within 5% for all the Ge and Te targets. The stronger deviation for Sn targets is explained by their larger non-uniformity (from 44 to 68%), as confirmed by the comparison of the FESEM microscopies of B4 (Sn) and B22 (Ge) samples shown in **Figure 3**. From these images the better uniformity of the Germanium deposition in B22 can be easily appreciated if compared with the topography of the Tin deposition of B4. This difference is confirmed by the R values measured by APT, that highlight the good thickness uniformity of the B22 Germanium deposition.

To evaluate how the target characteristics affect the NUMEN energy resolution, a Monte Carlo code has been implemented, which simulates the DCE events and estimates the ejectiles energy distribution using the experimental measurements as input (Pinna et al., 2020b).

Uncertainties on the average target thickness will affect the measured DCE cross section while the non-uniformity will affect the energy resolution on the DCE reaction products. A typical thickness uncertainty of 5% can be expected from the thickness measurement itself, performed with APT or RBS. An additional systematic uncertainty of typically a few % from the energy loss model should also be considered. A total uncertainty on the average thickness of 6–7% can therefore be foreseen, which will affect directly the measured cross section. However, since the cross section is proportional to the square of the NME, the corresponding contribution to the NME uncertainty will be about a factor two smaller.

To illustrate the effects of the target non-uniformity on the energy resolution of the DCE reaction products, we consider depositions on a 2 μm thick HOPG backing and DCE reactions at 15 MeV/u. With the characteristics of the Ge and Te target prototypes presented in **Table 2**, i.e., an average thickness of ≈ 400 nm and a non-uniformity R ≈ 10%, the contribution to the energy resolution due to the target non-uniformity would be quite small [≈80 keV Full Width at Half Maximum (FWHM)] leading to an overall FWHM of ≈460 keV. Therefore, the present Ge and Te uniformity appears to be acceptable. Considering a Sn target with a thickness of ≈200 nm, the contribution to the resolution due to the measured non-uniformity (R ≈ 60%) would be ≈300 keV, for an overall estimated resolution of ≈ 510 keV. The latter value is comparable to the excitation energy of the first excited state of the residual nucleus, thus increasing the Sn thickness to typical values of 600–700 nm would not be feasible. Additional investigations are required to improve the uniformity of the Sn depositions.

More studies are currently ongoing, on one side, to improve the deposition technique of Sn and, on the other side, to extend the APT and RBS tests to the other targets of the NUMEN foreseen experiments.

Enhancement of MAGNEX Magnetic Elements

A key item for the accomplishment of the NUMEN project is the upgrade of MAGNEX optical elements to higher magnetic rigidity to allow the transport of ions at higher energy. In particular, to match the request of the NUMEN experimental program, the magnetic field has to be increased of about 20% from the presently achievable highest values, preserving the present magnetic field maps, important for the application of ray reconstruction techniques (Lazzaro et al., 2007, 2008a,b, 2009). The expected new maximum fields will be 1.380 T (+20%) for the dipole magnet and 1.139 T (+20%) for the quadrupole one.

The evaluated field in the central region of the medium plane of the dipole magnet is plotted in **Figure 4** as a function of the excitation current. The first blue dot represents the field at the maximum current supplied by the present power supply (920 A), while the red dot is the new maximum field of 1.38 T achievable with a circulating current of 1,160 A (+26%) in the existing pair of coils (120 turn per coils). The higher circulating current means about 59% more power dissipation with respect to the present. A significant upgrade of the cooling of the magnets coils is thus needed. The usual constraint to maintain the coils at maximum temperature of 70°C requires the increase of the water inlet pressure up to 8 bar, preserving the present cooling circuit. In this way, the water flow is enough to dissipate the higher thermal power and keep the water temperature rise below the safe value of 20°. Nonetheless, the higher pressure also means a higher speed of the water flow, which could reduce the coils life due to the mechanical abrasion of the copper from the inner surface of the coil. To mitigate this problem, a dedicated cooling circuit at 8 bar will be used only when higher current is needed while the existing circuit at 5 bar is used at lower currents.

An inspection of **Figure 4** makes it clear that raising the excitation current in the dipole coils does not generate a linear increase of the magnetic field, due to the saturation of parts of the magnet iron. Finite element calculations of the magnetic fields generated by the bending magnet show that almost all

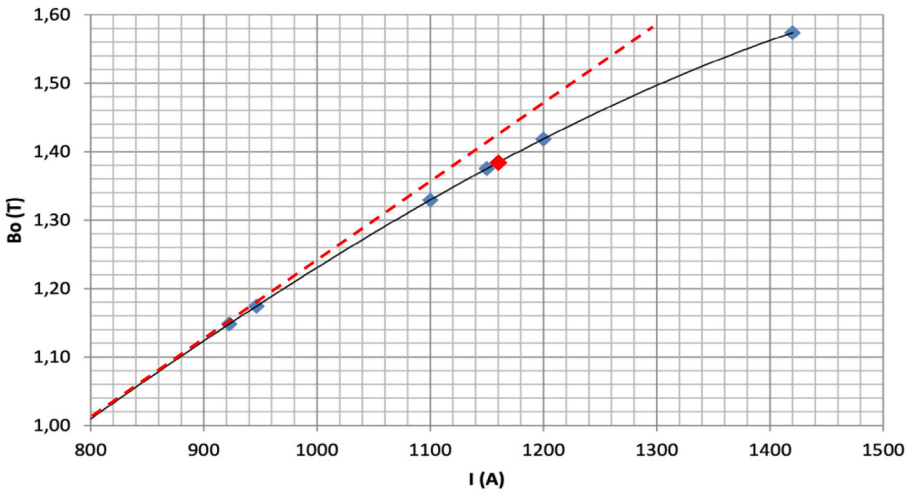

FIGURE 4 | Simulated field in the center of the dipole magnet as function of the excitation current. The red straight line emphasizes the deviation from linearity of the excitation curve.

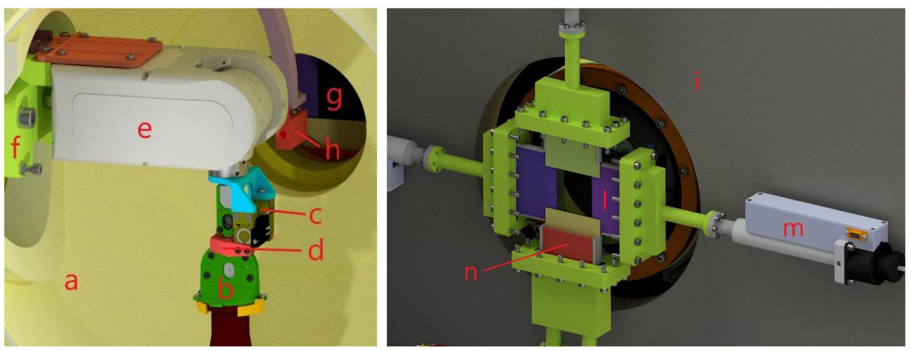

FIGURE 5 | Left: detail of the target manipulator end-effector. Inside the scattering chamber (a) the target-holder is connected to the cryo-cooler (b). A gripper (c) with its fingers (d) is used to disconnect the target-holder, which is rotated by a wrist (e) in horizontal position, then a pneumatic cylinder (f) moves the structure outside the chamber. During the automatic procedure, the Faraday cup (h) is aligned to the direction of the beam line in front of the slits system (g). Right: detail of the motorized slits system defining the MAGNEX acceptance at the entrance of the quadrupole magnet. The slits system is positioned upstream of the quadrupole shield (i) and it is composed by four screens (l) each one equipped with a linear drive (m). The "pepperpot" (n) is included in the lower part of this system.

the corners of the pole and part of the outer return yoke reach the saturation value of about 2 T. Because of saturation, the magnetic field over the pole surface is less uniform than at lower excitation. The existing MAGNEX surface coils will be used (Cunsolo et al., 2002; Cappuzzello et al., 2016) to compensate for the quadrupole (surface α-coil) and sextupole (surface β-coil) effects of the magnetic field at higher fields.

As also discussed in Section The new focal plane detector chamber, the MAGNEX surface α-coil has a key role for NUMEN, as it can generate a tunable positive or negative quadrupole-like field which effectively changes the focusing properties of the spectrometer, thus guaranteeing the fine focusing of the ejectiles onto the fixed FPD, according to the reaction kinematics (Cunsolo et al., 2002). However, due to the enhancement of the main field, also the surface coils need to be upgraded by allowing more current to flow through them and consequently more cooling. A detailed project for surface coils refurbishing in under way.

Finite elements simulations of the field distribution on the quadrupole magnet indicate that increasing the excitation current to 1,500 A (+50% with respect to the present maximum value), so as to achieve the requested gradient of 5.98 T/m (+20%), a sizable increase of the saturation is found. A further analysis of the high-order harmonics ($n > 2$) content in the field generated by the quadrupole magnet reveals that the main contribution comes from the $n = 6$ component, whose integrated strength is about 0.26% compared to the $n = 2$ and the trend is decreasing at increasing currents. Resembling the situation presented for the dipole magnet, also for the quadrupole an upgraded cooling system is demanded to remove the extra heat from the coils. A similar solution will be adopted with a complementary cooling system working at inlet pressure of 8 bar,

to maintain the water temperature increase below 20°C, to be used only when the experimental conditions require the highest excitation currents.

Due to the high-power request by the power supplies for the dipole and quadrupole magnets, 350 and 540 kW respectively, the overall electromagnetic noise induced by these elements could significantly interfere with sensitive electronic devices working in the MAGNEX hall. In particular, high sensitive charge pre-amplifiers coupled to the FPD detectors, are affected by high frequency components (>10 kHz) of the noise. Specific tests with different kinds of power supplies have been performed to characterize different sources of high-frequency electromagnetic induced and conducted noise. Results compliant with NUMEN specifications were found only with linear power supplies with series transistor banks. Based on these results, new power supplies with currents and voltages of 1,250 A, 280 V and 1,500 A, 360 V need to be built for the dipole and quadrupole magnets, respectively.

A New Scattering Chamber

A new scattering chamber matching the physics goal of the NUMEN experiment is under design according to the requirements coming from the upgrade of the MAGNEX spectrometer. As a main condition the chamber must cope with high intensity beam (10^{13} pps) still leaving the possibility to work with lower intensity beams (10^{11} pps).

To meet this request, two alternative beam lines, positioned at an angle of 70° to each other and pointing to the object point of the spectrometer, are foreseen. The scattering chamber, installed on the MAGNEX rotating platform, can be alternatively connected to each of the beam lines.

Additional rotations of the MAGNEX spectrometer with respect to the two beam line directions are obtained with two different mechanical systems according to the angular range to be explored in the NUMEN experiments. In the case of high intensity beams, a suitable mechanical bellows guarantees small rotations around two fixed angles (+3° and −3°) of the spectrometer optical axis. For low intensity beams, a sliding seal window allows continuous rotation of the optical axis in the −5–+25° angular range. Both systems guarantee to keep the high vacuum (10^{-6} mbar) in the chamber requested by the experiments. Inside the chamber, the target is supported by a holder, about 100 mm height, made of copper and shaped to include also slots for the beam monitoring devices. It should be noticed that the axis of the scattering chamber corresponds to the MAGNEX supporting platform fulcrum and, whatever chamber rotation is obtained, the target will be keeping its position, offering its surface to the normal incidence of the ion beam.

The target holder (Sartirana et al., 2020) is mounted over the cold finger of a vertical cryo-cooler, which maintains it at low temperature (∼40 K). A specific actuator below the cryo-cooler guarantees the movement of the target holder and fine alignment of the target to the beam axis (<200 μm).

Since a not negligible radiation level is foreseen in the scattering chamber, a significant activation of the target and its frame is expected, making its automatic handling necessary. A manipulator has been studied (Sartirana et al., 2020) in order to be placed outside the chamber at 90° with respect the beam line. The device is provided with a wrist featuring two degrees of freedom and when in position it clamps the target holder by the help of a pneumatic gripper and rotates it to disconnect from the cold finger (**Figure 5**-left). A bayonet coupling between the target holder and the cold finger facilitates the automatic procedure. A temporary storage outside the scattering chamber is used to collect up to 6 different targets.

The products from beam-target interactions are preferentially emitted in the forward direction together with the unreacted beam. A dedicated system, downstream the target, composed of two pairs of motorized slits, is implemented to further define the aperture of the spectrometer both in vertical and horizontal directions by limiting its acceptance within a maximum of ±7.5° in vertical direction and ±6.5° in horizontal one. The slits are made of 2 mm thick tantalum, each one controlled by a dedicated linear driver. The right panel of **Figure 5** shows the 3D CAD drawing of the motorized slit system. In addition, immediately upstream of the slit system, a "pepperpot" screen can be inserted by a dedicated linear driver along the beam for trajectory calibration purposes. It is made of tantalum and it features a matrix of holes 13 x 5, each of 1 mm diameter.

A Faraday cup (**Figure 5**-Left) has to be installed in the chamber for beam diagnostics purposes and to measure the integrated charge of the ion beam in the low intensity configuration. The system is inserted by the top of the scattering chamber and it is rotated in the measurement position (i.e., 0°) only if needed, otherwise it is kept at one side.

To keep the vacuum inside the chamber, the described components require static or dynamic sealing, with the further condition to guarantee an adequate radiation tolerance. This is obtained by applying rings of copper, elastomer or specific solutions as Helicoflex seals.

The New Focal Plane Detector Chamber

A challenging mechanical component for NUMEN is the new vacuum chamber containing the new FPD. A 3D model of these elements is shown in **Figure 6**. The chamber is coupled to the dipole magnet chamber by a large rectangular gate valve (800 × 230 mm internal clearance) to separate the magnets and focal plane volumes when different residual pressures are needed. This component also ensures the interchangeability of the new chamber with the existing one in MAGNEX.

Resembling the present chamber of the MAGNEX FPD (Torresi et al., 2021), the height of the new one will be kept larger than 230 mm to avoid interference with ion trajectories. On the other hand, the new chamber will have a larger width to allow both the ^{18}O and ^{20}Ne unreacted ion beams to be transported out of the spectrometer toward the beam dump lines, located besides the FPD. To guarantee the transmission of heavy ions toward the FPD and of the beam toward the beam dump lines a residual pressure in the range 10^{-5}-10^{-6} mbar has to be preserved.

The vacuum chamber houses the FPD that is filled with isobutane, featuring an absolute pressure of few tens of mbar. Specific internal walls separate the gas-filled region of the FPD from the chamber lateral regions under vacuum where the unreacted ion beams are directed toward the beam dump lines. A

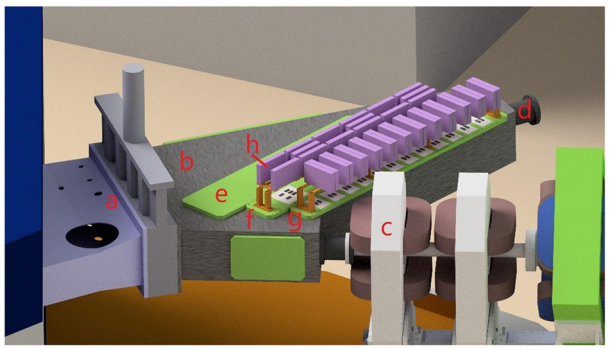

FIGURE 6 | The new design of the MAGNEX FPD. The gate valve at the dipole exit **(a)** is connected to the new FPD chamber **(b)**. This structure connects alternatively with ^{20}Ne and ^{18}O beam dump lines [**(c,d)**, respectively]; here the ^{20}Ne beam dump line configuration **(c)** is shown. On the top of the chamber three different flanges are present: one for the FPD Mylar window maintenance **(e)**, the second for the tracker and its electronics **(f)**, the last one for the PID wall **(g)**. The boxes on the top of these flanges contain the preamplifier circuits **(h)**.

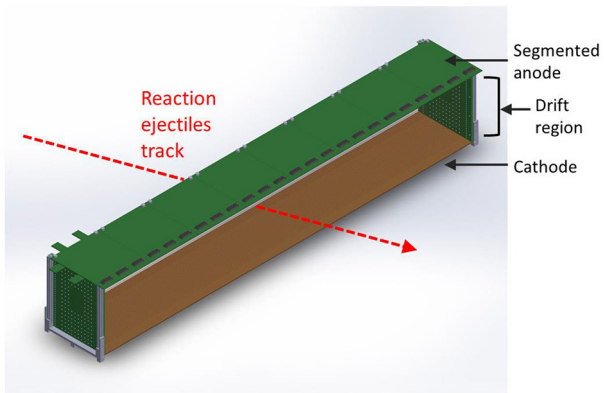

FIGURE 7 | Rendering of the full-size tracker cage that will be installed in FPD chamber.

very thin (few μm) Mylar window contains the isobutane within the FPD minimizing the material along the paths of the ions entering in the FPD. The FPD entrance window is tilted with an angle of 59° from the rectangular gate valve.

The window will be 150 mm high, and 920 mm large, thus slightly shorter than for the present detector (200 × 920 mm) (Torresi et al., 2021), reducing the overall ejectile transmission efficiency by about 10%. This guarantees compliance with the new FPD geometry (see Section The FPD gas tracker), and with the constraint from the beam transport outside the FPD chamber.

Contrary to the present FPD, the new one is not designed to move along the optical axis due to the mechanical limitation imposed by the first magnetic elements of the two beam dump lines. This prevents the possible fine focusing of the reaction products, by moving the FPD along the optical axis direction depending on the specific reaction kinematics (Cunsolo et al., 2002). Instead, as discussed in Section Enhancement of MAGNEX magnetic elements, the fine focusing of the reaction products is performed using the MAGNEX dipole surface α-coil (Cunsolo et al., 2002).

The new gas tracker and PID system, which constitute the active elements of the FPD (see Sections The FPD gas tracker and The particle identification system) are suspended to metal flanges sealed on the vacuum chamber top. Short coaxial cables are routed toward the detectors inside the FPD through SAMTEC multipin connectors, soldered on PCB boards present on each flange. This allows for independent and fast extraction and insertion of both systems from the chamber in case of need. Pre-amplifiers (CAEN MOD. 1429) are positioned on the top of these supporting flanges, outside the vacuum region. Long coaxial cables connect the front-end electronics to the read-out based on CAEN VX2740 multichannel digitizers (Finocchiaro et al., 2020). For the maintenance, each flange with pre-amplifiers circuits and suspended detectors will be hooked and lifted by a dedicated lifting system, positioned on board of the MAGNEX platform, in order to be placed on a stand near the spectrometer. The same lifting system will work on a third flange on the top of the vacuum chamber that allows the installation of the mylar window.

The FPD Gas Tracker

The aim of the FPD-gas tracker is to provide a precise and accurate three-dimensional tracking of the particles crossing the focal plane. Two characteristics for the gas tracker are required by the NUMEN project.

The first is a high resolution measurement of the phase space parameters of the ion tracks at the focal plane: X_{foc}, Y_{foc}, θ_{foc}, ϕ_{foc}, where X_{foc} is the horizontal coordinate (dispersive direction in the focal plane), θ_{foc} the horizontal angle, Y_{foc} the vertical coordinate and ϕ_{foc} the vertical angle. The required resolution is lower than 0.6 mm that for X_{foc} and Y_{foc} and lower than 5 mr for θ_{foc} and ϕ_{foc}. This requirement is of fundamental importance because the precise and accurate particle ray reconstruction is mandatory for the determination of the momentum vector at the target position that, in turn, translates in scattering angle and particle energy.

The second requirement is to withstand the expected high rate of impinging particles. The particle rate density along the 92 cm horizontal aperture of the FPD at full intensity is foreseen to be about 50 kHz/cm. The tracker should be able to cope with such a high rate managing to disentangle the track of each detected particle and maintain the required resolutions on the phase space parameters. For that reason, particular care has been devoted to the choice of the multiplication stage. Among all the Micro-Pattern Gas Detector types (MPGD), the multiple THick Gas Electron Multipliers (THGEM) have been chosen because, based on PCB technology, they are mechanically robust, easy to build and to handle, and economical. Moreover, the choice of multiple THGEM in place of a single one is motivated by the higher gain achievable at fixed operational voltage, which allows to reduce the voltage thus ensuring a better stability and longer average life.

The working principles of the adopted solution and first results from a reduced size prototype of the tracker can be found in Finocchiaro et al. (2020). As the focus of the present article is on recent advancements, two aspects need to be specifically

considered. First, a new full-scale project of the tracker assembly, based on the prototype adopted solutions, is now available, as shown in **Figure 7**.

The volume of the new detector, filled with gas (e.g., isobutane at a typical pressure of few tens of mbar), will be 1,200 × 185 × 118 mm^3. When an ionizing particle crosses the volume it generates a track of primary electrons and positive ions. Under the effect of a uniform electric field, the electrons drift, at constant velocity, toward the multiplication stage that is based on multiple THGEM (Sauli, 2016; Cortesi et al., 2017) that can easily cope with the expected rate of particles. The strong electric field inside the THGEM induces charge multiplication, generating electron jets, which are directed toward the anode.

Second, a new anode, segmented in small pads with size of 5 × 10 mm^2 was designed and is presently under construction. Compared to the previous anode the new one allows for an easier track reconstruction, especially at high rate, where ambiguities to the assignment of the detector signals to a specific event could be an important issue. **Figure 8** shows a sketch of one of the four modules which will be mounted side-by side in the new anode. The pads are arranged in five rows each one made of more than 200 units. Neighboring rows of pads are spaced by 10 mm. In this way the ion track is sampled in five positions inside the tracker. Knowing which pads are hit by the electrons and the total collected charge it is possible to extract the two-dimensional projection of the track on the horizontal plane X-Z with a submillimeter precision. The vertical coordinate Y_{foc} is determined by the measurement of the electron drift times. This corresponds to the interval between the signal-over-threshold time generated by the ion on a SiC detector (see Section The particle identification system) and the signal-over-threshold time generated by secondary electrons on the anodic pads. In this way a full three-dimensional track is obtained on an event-by-event basis.

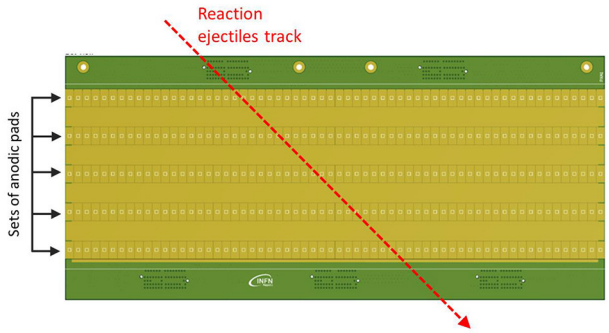

FIGURE 8 | CAD drawing of one module of the new anode of the MAGNEX FPD for NUMEN.

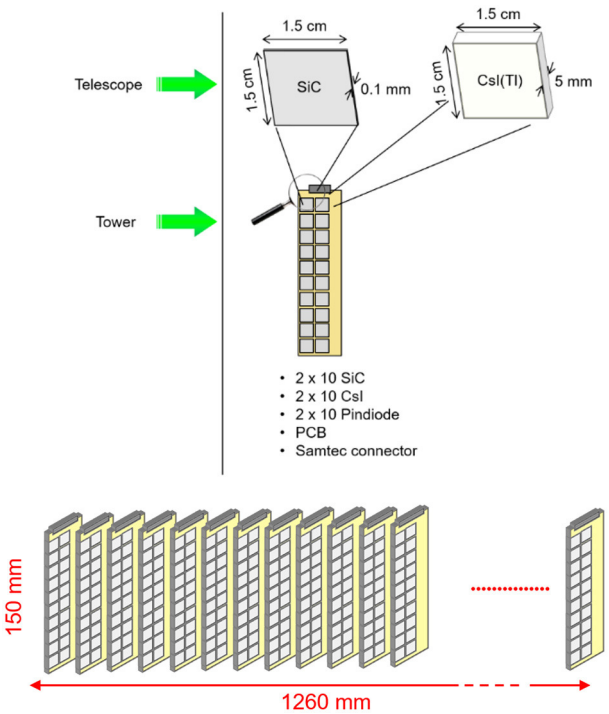

FIGURE 9 | Top: mechanical arrangement of the PID detector telescopes. The telescopes are arranged into *towers*, each one consisting of 20 units. Bottom: mechanical arrangement of the PID *towers*. The full focal plane is covered by 36 towers rotated by 35° around the vertical axis (see text).

The Particle Identification System

The ejectiles to be identified in the NUMEN experiments are typically in the mass region $10 < A < 25$ and atomic number $4 < Z < 12$. Due to the interaction with the target (Cavallaro et al., 2019), ions characterized by different charge states (q) are distributed at the focal plane for each isotope species, making the ion identification more challenging. The adopted technique for particle identification (PID) with MAGNEX, described in Cappuzzello et al. (2010), Calabrese et al. (2018), guarantees a clear selection of the ions of interest in the whole range of A and Z produced in the collision, provided that precise measurements of the energy loss (ΔE), the residual energy (E_r) and the horizontal position at the focus (X_{foc}) are available.

In the new MAGNEX FPD, the gas tracker will provide accurate measurement of the X_{foc} parameter, while ΔE and E_r are obtained from a dedicated array of two-stage telescopes of Silicon Carbide (SiC) (Tudisco et al., 2018) and Tallium doped Cesium Iodide CsI(Tl) detectors. The active area of each element is 1.5 × 1.5 cm, with 0.2 mm dead space between adjacent cells. The SiC detector is 100 μm thick and measures ΔE. The CsI(Tl) inorganic scintillator is 5 mm thick and is coupled to a Hamamatsu S3590 photodiode of 1 × 1 cm area to measure E_r.

The capabilities of the system in terms of radiation hardness and mass resolution are discussed in Finocchiaro et al. (2020). A new mechanical arrangement of the telescopes is presented here, as a result of optimization of the detection efficiency and the mechanical integration. Indeed, in the configuration shown in Finocchiaro et al. (2020), the central region of the vertical coordinate (Y_{foc}∼0) was not covered as it corresponded to the dead region between two vertical modules. This would have determined a relevant efficiency loss, since close to the MAGNEX symmetry plane ($Y_{foc} \sim 0$) the ion rate is maximum (see for e.g.,

Cappuzzello et al., 2014; Carbone, 2015). For this reason, in the new geometry, shown in **Figure 9**, the telescopes are arranged in *towers* (10 rows and 2 columns each) in order to avoid efficiency losses for $Y_{foc} \sim 0$. From the mechanical point of view, with this new configuration the towers can be precisely mounted and easily attached on the top flange of the FPD chamber (see Section The new focal plane detector chamber) by means of a mechanical stand, making also the mounting and maintenance procedures more comfortable. A PCB board houses the pin diodes on top of which CsI(Tl) crystals are glued. A copper grid is placed on the top of the crystals over which the SiC detectors can be glued. The signals are collected and sent to the front-end electronics (Caen V1429 64-channel pre-amplifiers) by means of a connector on the top of each tower (see **Figure 9**-top). The readout is performed using 64-channel digitizers (Caen VX2740), as described in Ref. (Finocchiaro et al., 2020). Since the MAGNEX FPD is rotated around the vertical axis by 59° with respect to the plane normal to the optical (Cunsolo et al., 2002), the towers are also rotated of about 35° around the vertical axis, in order to minimize the differences in the path length inside the detectors. GEANT4 simulations show that such an arrangement moreover avoids that unwanted neutron and γ-ray fluxes, produced by the interaction of the ejectiles with one SiC-CsI(Tl) telescope, could interfere with the telescope beyond. With the present geometry the full length of the FPD will be covered by 36 PID towers, placed downstream of the tracker, for a total of 720 telescopes.

The G-NUMEN Gamma Spectrometer Array

The typical energy resolution for a NUMEN experiment is around 500 keV (FWHM) at 15 MeV/u beam energies, which is sufficient for the separation of the low-lying excited states and ground state of the fragments of the DCE reaction in some near-spherical target mass regions. However, this is not the case for deformed nuclei, for which the low-lying states appear well-below 500 keV, and for all cases at high beam energies (around 30 MeV/u or above) since there is a significant contribution from the accelerated beam energy resolution itself (0.1%) and from the MAGNEX optics (0.1%). To allow for the separate determination of the cross sections of the ground-state and first excited states of both the projectile (PLF) and the target (TLF) fragments of the DCE nuclear reaction, an array of gamma-ray detectors will be used (Oliveira et al., 2018). The gamma rays will be detected in coincidence with the PLF, identified at the MAGNEX focal plane. With an energy resolution at least one order of magnitude better than the best ones achievable with MAGNEX under NUMEN experiment conditions, it should be possible to separate the close-to-ground state transitions and therefore measure their cross sections.

This gamma array must fulfill a series of requirements, besides guaranteeing sufficient energy resolution. It should have a high photo-peak detection efficiency, due to the minute DCE cross sections expected, the detectors should be tolerant to a high radiation field of gamma rays and neutrons, due to the interaction of high intensity beam with the target and tolerate high counting rates. The timing resolution should also be high enough to clearly separate events from subsequent accelerated beam bunches. In order to meet those requirements, an inorganic scintillator array

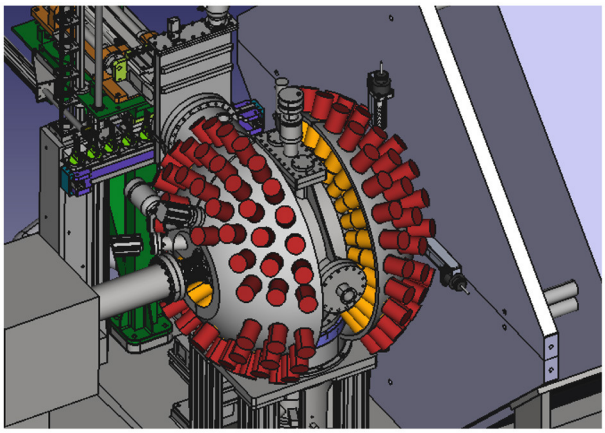

FIGURE 10 | The G-NUMEN gamma spectrometer disposed around the MAGNEX scattering chamber.

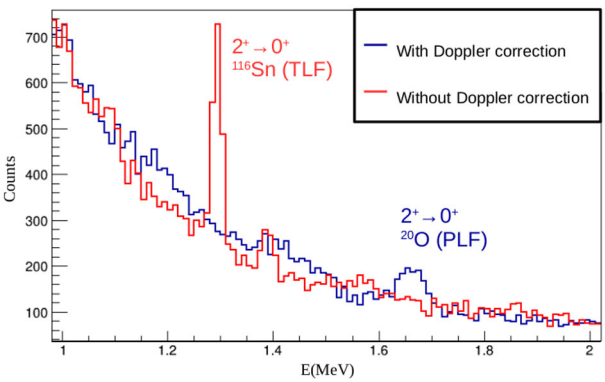

FIGURE 11 | Simulation of the G-NUMEN γ-ray spectra for transitions to low-lying states of a typical DCE experiment.

with large angular coverage (as high as possible, given the limitations imposed by the peripheral equipment around the scattering chamber) and high granularity, to control pulse pile up, was envisaged. The $LaBr_3$(Ce) scintillator was chosen among inorganic scintillators due to its high radiation tolerance and fast timing response, high photopeak intrinsic efficiency and excellent energy resolution. The scintillator crystals will be coupled to standard photomultiplier tubes due to the fast response and good radiation tolerance of these devices. **Figure 10** presents a CAD sketch of the gamma detector array, mounted around the scattering chamber.

The dimensions of the crystals will be 38 mm diameter and 50 mm length, and their faces will be at about 245 mm distance from the target. The detectors will be disposed in rings between 43 and 149 degrees to the beam direction, covering a total solid angle of 20% of the unit sphere. The expected total photopeak efficiency of the array will be near 4%, and the energy resolution around 3%, at 1.3 MeV gamma-ray energy. The expected timing resolution should be under 1 ns. This is important to separate

the PLF-gamma coincident events from the huge background of gamma rays from all other nuclear reactions with the beam and target combination of the experiment.

Extensive GEANT4 simulations (Agostinelli et al., 2003; Folger et al., 2004; Allison et al., 2006, 2016; Oliveira et al., 2020), based on the BIC (binary intra-nuclear cascade) model of the reaction were performed in order to evaluate this background. The results indicate that cross sections as low as 1 nb, can be measured with uncertainties of the order of 10%, using a beam intensity of the order of 10^{12} beam particles per second on typical targets with tenths of mg/cm^2 surface density in month-long experiments. Typical gamma count rates of 300 kHz are expected for each detector. The beam intensity is limited to that order of magnitude by pile-up effects and simultaneous occurrence of more than one nuclear reaction within the same beam pulse, which makes the gamma event time virtually undistinguishable.

Figure 11 presents the simulated gamma-ray spectra for the reaction case of ^{116}Cd(^{20}Ne,^{20}O) at 300 MeV. It illustrates the presence of background under the transitions from the first excited states of the target-like fragment (TLF) and the projectile-like fragment (PLF—with Doppler correction which is quite significant for this case), at the high beam current conditions. This background is comparatively negligible at low beam currents. The data acquisition will be performed with CAEN digitizers (VX2740). The possibility to do on-line particle-gamma coincidences with these modules is being explored in view of possible mitigation of data storage space issues during experiments.

Radiation Level

The knowledge of the radiation level expected inside the MAGNEX experimental hall is of paramount importance since high rates of neutron and gamma-rays could spoil the performance of the electronic devices and of the detectors used in the MAGNEX FPD. Dedicated Monte Carlo simulations for the radiation background at the MAGNEX facility have been performed using the FLUKA code (Ferrari et al., 2005; Vlachoudis, 2009; Bohlen et al., 2014). A schematic geometry of the experimental room was implemented in the simulations as shown in **Figure 12**. In the present study, three main radiation sources were considered, namely:

- The interaction of the beam particles with the target material
- The interaction of beam particles with the beam stopper inside the beam dump
- A hypothetical 10W power loss in the beam intensity along the beam line. This is a conservative assumption (0.5% of the maximum beam power) to describe the possible source of radiation represented by the interaction of beam halos with the vacuum pipes of the magnetic elements located at the exit of the FPD (see Section The new focal plane detector chamber).

The simulation was performed following the prescription of Ref. (Lo Presti et al., 2020). In more details, a ^{20}Ne^{10+} beam at the energy of 60 MeV/u with an intensity of 2 kW ($\sim 1 \times 10^{13}$ pps) was directed onto a 214 μg/cm^2 thick ^{76}Ge target followed by a 2 μm thick ^{12}C layer. The simulated neutron flux, measured at the FPD (see **Figure 12**), is presented in **Figure 13** with the dashed green-line. Further on, a loss of 10 W along the beam line toward the beam dump was also considered in our simulations. This loss is assumed to occur at the position where the second steerer magnet will be installed (indicated with a blue cross in **Figure 12**). In this case, a substantial increase in the radiation level in the vicinity of the FPD is found. In the last part of our simulations, the ^{20}Ne beam was directed into the beam dump, stopped in a thick Ag target. The beam dump is confined into a (5 × 5 × 3) m^3 Portland concrete cube, providing thus an effective shield against neutron and gamma radiation.

Considering the contribution of the radiation sources mentioned above, the distribution of the simulated neutron flux

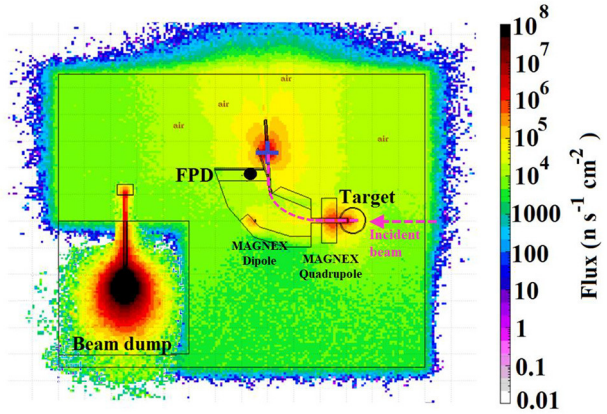

FIGURE 12 | Estimated neutron flux inside the MAGNEX experimental hall via FLUKA simulations. The result is obtained considering three radiation sources namely the beam-target interaction, the beam dump and a 10W loss of the beam power close to the MAGNEX FPD. The detector used in the simulation is indicated by a filled black circle, while the position where the 10 W loss occurs is indicated with the blue cross (see text for details).

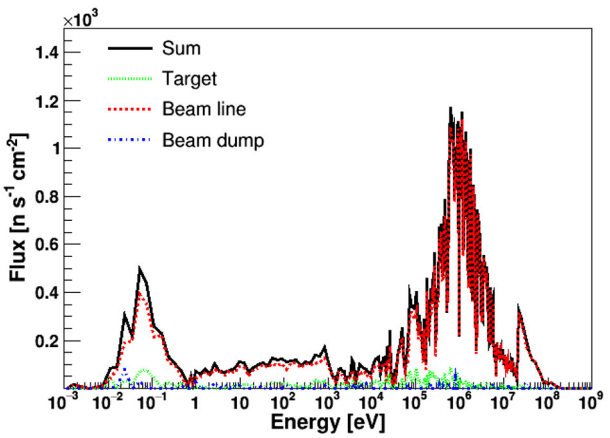

FIGURE 13 | Simulated neutron energy spectra at the MAGNEX FPD region. The contributions from the beam-target interaction, the beam dump and the 10W loss along the beam line are denoted by the dotted green, dotted-dashed blue and dashed red lines, respectively. The sum of the three contributions is presented with the solid black line.

inside the experimental hall is given in **Figure 12**, while the corresponding energy spectra are shown in **Figure 13**. The total integrated neutron flux is $7.2*10^4$ $n*s^{-1}*cm^{-2}$, dominated by fast neutrons above 100 keV.

Both **Figures 12**, **13** show that the main contribution to the neutron flux in the FPD region comes from the possible scattering of the beam into the beam pipe close to the FPD. Therefore, a detailed study of the beam transport is in progress in order to quantify the beam losses in such area and reduce them to tolerable values. Moreover, a substantial reduction of the neutron flux is expected by the introduction of proper shields to the detectors and electronics, which are also presently under study.

CONCLUSION AND PERSPECTIVES

Pioneering experimental campaigns, using the (^{18}O,^{18}Ne) and (^{20}Ne,^{20}O) DCE reactions on a few isotope candidates for 0νββ-decay, have been recently performed at INFN-LNS Laboratory by the NUMEN collaboration. The data analysis is ongoing, with preliminary results showing that accurate DCE cross sections measurements can be extracted at very forward angles for the ground-to-ground state transitions. In the experiments a wide net of direct reactions, generated by the beam-target interaction was also explored, providing additional information useful to characterize the complicated many-body nature of the involved nuclei as well as the reaction mechanisms.

The measurement of DCE absolute cross sections and the extraction of relevant NMEs is the main objective of the NUMEN project. An ambitious goal of NUMEN is to investigate the link between NMEs extracted from DCE reactions and those characterizing 0νββ decay. In this perspective, NUMEN is proposing an original experimental and theoretical approach to 0νββ decay NMEs that could contribute to the extraction of the absolute value of neutrino average mass from the expected observation of this rare decay.

The systematic exploration of all 0νββ decay candidate isotopes is highly desirable for neutrino physics and NUMEN is fully committed to pursue this ambitious goal. However, despite the first promising results achieved to date, much remains to be done toward the determination of NME for 0νββ decay, with the necessary accuracy to foster the neutrino physics.

As described in this paper, the project promotes a major and widely distributed upgrade of the INFN–LNS research facility in view of a significant increase of the beam intensity. As a consequence, several aspects of the technology involved in heavy ion collision experiments demand for challenging R&D.

The acceleration of heavy ion beams required by the NUMEN experiments in the regime of kW power and at energies from 15 to 70 MeV/u leads to substantial changes in the adopted technologies to extract the beam from the INFN-LNS Superconducting Cyclotron. The transport of such beams poses important radioprotection issues which requires a careful evaluation of radiation levels also involving the effects on detectors, electronics and various equipment. A critical aspect is the design of isotopically-enriched, thin and uniform targets for DCE experiments, considering the deterioration due to the dissipation of the enormous amount of heat deposited by the ion beam. The copious production of reaction products emerging from the target makes the present detectors of the MAGNEX spectrometer unfit for this application. A dedicated study of new classes of detectors, coping with the expected high rate and high fluency, still preserving the high resolution and sensitivity of the present ones is mandatory. This includes the search of new materials, the study of new electronics and DAQ systems, matching the rather stringent experimental requests and a complex mechanical integration of all parts, accounting for the limitation on human activities in the experimental hall due to radioprotection issues. Such R&D activity is a fundamental aspect of the NUMEN project, already supported by INFN to move to its construction phase.

In perspective, NUMEN aims at giving an innovative contribution in one of the most promising fields of fundamental physics. It indicates also a new avenue for heavy ion physics in synergy with neutrino physics with possible fallout in other research fields as well as in technological developments.

DATA AVAILABILITY STATEMENT

The raw data supporting the conclusions of this article will be made available by the authors, without undue reservation.

AUTHOR CONTRIBUTIONS

All authors listed have made a substantial, direct and intellectual contribution to the work, and approved it for publication.

FUNDING

The NUMEN project is mainly funded by INFN. Additional funds come from the Italian Ministry of University and Research (MIUR) under the *FARE Ricerca in Italia* program, with grant number R16HXFTMCT and acronym TEBE (SC and MF contracts are paid under TEBE). This project has also received funding from the European Research Council (ERC) under the European Union's Horizon 2020 research and innovation program, NURE project, grant agreement No. 714625 (The contracts of DT and FD are totally paid under NURE. The contracts of MC and FC are partly paid under NURE). JO acknowledges support from Fundação de Amparo à pesquisa no Estado de São Paulo, (FAPESP SPRINT grant proc. 2017/50160-5). LA and EC acknowledge support from DGAPA-UNAM IN107820, AG101120, and CONACyT 314857.

REFERENCES

Agodi, C., Cappuzzello, F., Cavallaro, M., Bondì, M., Carbone, D., Cunsolo, A., et al. (2015). Heavy ions double charge exchange reactions: towards the 0νββ nuclear matrix element determination. *Nucl. Part Phys. Proc*. 265, 28–30. doi: 10.1016/j.nuclphysbps.2015.06.007

Agodi, C., Russo, A. D., Calabretta, L., D'Agostino, G., Cappuzzello, F., Cavallaro, M., et al. (2021). The NUMEN project towards new experiments with high intensity beams. *Universe* 7:72. doi: 10.3390/universe7030072

Agostinelli, S., Allison, J., Amako, K., Apostolakis, J., Araujo, H., Arce, P., et al. (2003). Geant4—a simulation toolkit. *Nucl. Instr. Method A* 506:250. doi: 10.1016/S0168-9002(03)01368-8

Allison, J., Amako, K., Apostolakis, J., Araujo, H., Arce Dubois, P., Asai, M., et al. (2006). Geant4 developments and applications. *IEEE Trans. Nucl. Sci*. 53:270. doi: 10.1109/TNS.2006.869826

Allison, J., Amako, K., Apostolakis, J., Arce, P., Asai, M., Aso, T., et al. (2016). Recent developments in Geant4. *Nucl. Instr. Method A* 835:186. doi: 10.1016/j.nima.2016.06.125

Barea, J., Kotila, J., and Iachello, F. (2013). Nuclear matrix elements for double-β decay. *Phys. Rev. C* 87:014315. doi: 10.1103/PhysRevC.87.014315

Bellone, J. I., Burrello, S., Colonna, M., Lay, J.-A., and Lenske, H. (2020). Two-step description of heavy ion double charge exchange reactions. *Phys. Lett. B* 807:135528. doi: 10.1016/j.physletb.2020.135528

Bohlen, T. T., Cerutti, F., Chin, M. P. W., Fassò, A., Ferrari, A., Ortega, P. G., et al. (2014). The FLUKA code: developments and challenges for high energy and medical applications. *Nucl. Data Sheets* 120:211. doi: 10.1016/j.nds.2014.07.049

Calabrese, S., Cappuzzello, F., Carbone, D., Cavallaro, M., Agodi, C., Acosta, L., et al. (2018). First measurement of the 116Cd(20Ne,20O)116Sn. *Acta Phys. Pol. B* 49:275. doi: 10.5506/APhysPolB.49.275

Calabrese, S., Cappuzzello, F., Carbone, D., Cavallaro, M., Agodi, C., Torresi, D., et al. (2020). Analysis of the background on cross section measurements with the MAGNEX. *Nucl. Inst. Method Phys. Res. A* 980:164500. doi: 10.1016/j.nima.2020.164500

Capirossi, V., Delaunay, F., Iazzi, F., Pinna, F., Calvo, D., Fisichella, M., et al. (2020). Thickness and uniformity characterization of thin targets for intense ion beam experiments. *Acta Phys. Pol. B* 51:661. doi: 10.5506/APhysPolB.51.661

Cappuzzello, F., and Agodi, C. (2021). The NUMEN project: shedding light on neutrinoless double beta decay by heavy-ion nuclear reactions. *Nucl. Phys. News*. 31. doi: 10.1080/10619127.2021.1881368

Cappuzzello, F., Agodi, C., Bondì, M., Carbone, D., Cavallaro, M., Cunsolo, A., et al.. (2014). A broad angular-range measurement of elastic and inelastic scatterings in the 16O on 27Al reaction at 17.5 MeV/u. *Nucl. Instr. Method A* 763:314. doi: 10.1016/j.nima.2014.06.058

Cappuzzello, F., Agodi, C., Bondì, M., Carbone, D., Cavallaro, M., and Foti, A. (2015a). The role of nuclear reactions in the problem of 0νββ decay and the NUMEN project at INFN-LNSJ. *Phys. Conf. Ser*. 630:012018. doi: 10.1088/1742-6596/630/1/012018

Cappuzzello, F., Agodi, C., Carbone, D., and Cavallaro, M. (2016). The MAGNEX spectrometer: results and perspectives. *Eur. Phys. J. A* 52:167. doi: 10.1140/epja/i2016-16167-1

Cappuzzello, F., Agodi, C., Cavallaro, M., Carbone, D., Tudisco, S., Lo Presti, D., et al.. (2018). The NUMEN project: NUclear matrix elements. *Eur. Phys. J. A* 54:72. doi: 10.1140/epja/i2018-12509-3

Cappuzzello, F., Carbone, D., and Cavallaro, M. (2011). Measuring the ions momentum vector with a large acceptance magnetic spectrometer. *Nucl. Instr. Method A* 638:74. doi: 10.1016/j.nima.2011.02.045

Cappuzzello, F., Carbone, D., Cavallaro, M., Bondì, M., Agodi, C., Azaiez, F., et al. (2015c). Signatures of the giant pairing vibration in the 14C and 15C atomic nuclei. *Nat. Comm*. 6:6743. doi: 10.1038/ncomms7743

Cappuzzello, F., Carbone, D., Cavallaro, M., Spatafora, A., Ferreira, J. L., Agodi, C., et al. (2021). Confirmation of giant pairing vibration evidence in 12,13C(18O,16O)14,15C reactions at 275 MeV. *Eur. Phys. J. A* 57:34. doi: 10.1140/epja/s10050-021-00345-7

Cappuzzello, F., and Cavallaro, M. (2020). Nuclear response to second-order isospin probes in connection to double beta decay. *Universe*. 6:217. doi: 10.3390/universe6110217

Cappuzzello, F., Cavallaro, M., Agodi, C., Bondì, M., Carbone, D., Cunsolo, A., et al. (2015b). Heavy-ion double charge exchange reactions: a tool toward 0nbb nuclear matrix elements. *Eur. Phys. J. A* 51:145. doi: 10.1140/epja/i2015-15145-5

Cappuzzello, F., Cavallaro, M., Cunsolo, A., Foti, A., Carbone, D., Orrigo, S. E. A., et al. (2010). A particle identification technique for large acceptance spectrometers. *Nucl. Instr. Method A* 621:419. doi: 10.1016/j.nima.2010.05.027

Cappuzzello, F., Lenske, H., Cunsolo, A., Beaumel, D., et al.. (2004). Analysis of the 11B(7Li, 7Be)11Be reaction at 57 MeV in a microscopic approach. *Nucl. Phys. A* 739, 30–56. doi: 10.1016/j.nuclphysa.2004.03.221

Carbone, D. (2015). Signals of the giant pairing vibration in 14C and 15C nuclei populated by (18O,16O) two-neutron transfer reactions. *Eur. Phys. J. Plus* 130:43. doi: 10.1140/epjp/i2015-15143-0

Carbone, D., Cappuzzello, F., and Cavallaro, M. (2012). Universal algorithm for the analysis of charge distributions in segmented electrodes of gas detectors. *Euro. Phys. J. A*. 48:60. doi: 10.1140/epja/i2012-12060-3

Carbone, D., Ferreira, J. L., Calabrese, S., Cappuzzello, F., Cavallaro, M., Hacisalihoglu, A., et al. (2020). Analysis of two-nucleon transfer reactions in the 20Ne+116Cd system at 306 MeV. *Phys. Rev. C* 102:044606. doi: 10.1103/PhysRevC.102.044606

Carbone, D., Linares, R., Amador-Valenzuela, P., Calabrese, S., Cappuzzello, F., Cavallaro, M., et al. (2021). Initial state interaction for the 20Ne + 130Te and 18O + 116Sn systems at 15.3 AMeV from elastic and inelastic scattering measurements. *Universe* 7:58. doi: 10.3390/universe7030058

Cavallaro, M., Aciksoz, E., Acosta, L., Agodi, C., Auerbach, N., Bellone, J. I., et al. (2017). "NURE: an ERC project to study nuclear reactions," in *Proceedings, 55th International Winter Meeting on Nuclear Physics Bormio*, (Bormio). doi: 10.22323/1.302.0015

Cavallaro, M., Agodi, C., Assie, M., Azaiez, F., Cappuzzello, F., Carbone, D., et al. (2016). Neutron decay of 15C resonances by measurements of neutron time-of-flight. *Phys. Rev. C* 93:064323. doi: 10.1103/PhysRevC.93.064323

Cavallaro, M., Agodi, C., Brischetto, G. A., Calabrese, S., Cappuzzello, F., Carbone, D., et al. (2020). The MAGNEX magnetic spectrometer for double charge exchange reactions. *Nucl. Inst. Method Phys. Res. B* 463, 334–338. doi: 10.1016/j.nimb.2019.04.069

Cavallaro, M., Bellone, J. I., Calabrese, S., Agodi, C., Burrello, S., Cappuzzello, F., et al. (2021). A constrained analysis of the 40Ca(18O,18F)40K direct charge exchange reaction mechanism at 275 MeV. *Front. Space Sci. Astron.*

Cavallaro, M., Cappuzzello, F., Carbone, D., Cunsolo, A., Foti, A., Khouaja, A., et al. (2012). The low-pressure focal plane detector of the MAGNEX spectrometer. *Eur. Phys. J. A* 48:59. doi: 10.1140/epja/i2012-12059-8

Cavallaro, M., Santagati, G., Cappuzzello, F., Carbone, D., Linares, R., Torresi, D., et al. (2019). Charge-state distributions of 20 Ne ions emerging from thin foils. *Res. in Phys*. 13, 102191. doi: 10.1016/j.rinp.2019.102191

Cortesi, M., Rost, S., Mittig, W., Ayyad-Limonge, Y., Bazin, D., Yurkon, J., et al. (2017). Multi-layer thick gas electron multiplier (M-THGEM): a new MPGD structure for high-gain operation at low-pressure. *Rev. Sci. Instr*. 88:013303. doi: 10.1063/1.4974333

Cunsolo, A., Cappuzzello, F., Foti, A., Lazzaro, A., and Melita, A. L. (2002). Ion optics for large-acceptance magnetic spectrometers. *Nucl. Instr. Method A* 484:56. doi: 10.1016/S0168-9002(01)02004-6

Dell'Oro, S., Marcocci, S., Viel, M., and Vissani, F. (2016). Neutrinoless double beta decay: 2015 review. *Adv. High Ener. Phys*. 2016:2162659. doi: 10.1155/2016/2162659

Ejiri, H., Suhonen, J., and Zuber, K. (2019). Neutrino-nuclear responses for astro-neutrinos, single beta decays and double beta decays. *Phys. Rep*. 797, 1–102. doi: 10.1016/j.physrep.2018.12.001

Engel, J., and Menendez, J. (2017). Status and future of nuclear matrix elements for neutrinoless double-beta: a review. *Rep. Progr. Phys*. 80:046301. doi: 10.1088/1361-6633/aa5bc5

Ferrari, A., Sala, P. R., Fassò, A., and Ranft, J. (2005). *CERN-2005-10, INFN/TC_05/11, SLAC-R-773*.

Ferreira, J. L., Carbone, D., Cavallaro, M., Deshmukh, N. N., Agodi, C., Brischetto, G. A., et al. (2021). Analysis of two-proton transfer in the 40Ca(18O,20Ne)38Ar reaction at 270 MeV. *Phys. Rev. C*.

Finocchiaro, P., Acosta, L., Agodi, C., Altana, C., Amador-Valenzuela, P., Boztosun, I., et al. (2020). The NUMEN heavy ion multidetector for a complementary approach to the neutrinoless double beta decay. *Universe* 6:129. doi: 10.3390/universe6090129

Folger, G., Ivanchenko, V. N., and Wellisch, J. P. (2004).The binary cascade. *Eur. Phys. J. A* 21:407. doi: 10.1140/epja/i2003-10219-7

Gouvea, A., and Vogel, P. (2013). Lepton flavor and number conservation and physics beyond the standard model. *Prog. Part. Nucl. Phys.* 71:75. doi: 10.1016/j.ppnp.2013.03.006

Iazzi, F., Ferrero, S., Introzzi, R., Pinna, F., Scaltrito, L., Calvo, D., et al. (2017). A new cooling technique for targets operating under very intense beams. *WIT Trans. Engin. Sci*. 116:61. doi: 10.2495/MC170071

Kisamori, K., Shimoura, S., Miya, H., Michimasa, S., Ota, S., Assie, M., et al. (2016). Candidate resonant tetraneutron state populated by the 4He(8He,8Be) reaction. *Phys. Rev. Lett*. 116:052501. doi: 10.1103/PhysRevLett.116.052501

La Fauci, L., Spatafora, A., Cappuzzello, F., Agodi, C., Carbone, D., Cavallaro, M., et al. (2021). 18O + 76Se elastic and inelastic scattering at 275 MeV. *Phys. Rev. C*.

Lazzaro, A., Cappuzzello, F., Cunsolo, A., Cavallaro, M., Foti, A., Khouaja, A., et al. (2007). Field simulations for large dipole magnets. *Nucl. Instr. Method A* 570:192. doi: 10.1016/j.nima.2006.10.055

Lazzaro, A., Cappuzzello, F., Cunsolo, A., Cavallaro, M., Foti, A., Orrigo, S. E. A., et al. (2008a). Field measurement for large quadrupole magnets. *Nucl. Instr. Method A* 591:394. doi: 10.1016/j.nima.2008.02.103

Lazzaro, A., Cappuzzello, F., Cunsolo, A., Cavallaro, M., Foti, A., Orrigo, S. E. A., et al. (2008b). Field measurement for large bending magnets. *Nucl. Instr. and Meth. A*. 585, 136. doi: 10.1016/j.nima.2007.10.046

Lazzaro, A., Cappuzzello, F., Cunsolo, A., Cavallaro, M., Foti, A., Orrigo, S. E. A., et al. (2009). Field reconstruction in large aperture quadrupole magnets. *Nucl. Instr. Method A* 602:494. doi: 10.1016/j.nima.2009.01.019

Lenske, H., Bellone, J. I., Colonna, M., and Lay, J. A. (2018). Theory of single-charge exchange heavy-ionreactions. *Phys. Rev. C* 98:044620. doi: 10.1103/PhysRevC.98.044620

Lenske, H., Cappuzzello, F., Cavallaro, M., and Colonna, M. (2019). Heavy ion charge exchange reactions as probes for nuclear beta-decay. *Prog. Part Nucl. Phys*. 109:103716. doi: 10.1016/j.ppnp.2019.103716

Lo Presti, D., Medina, N. H., Guazzelli, M. A., Moralles, M., Aguiar, V. A. P., Oliveira, J. R. B., et al. (2020). Neutron radiation effects on an electronic system on module. *Rev. Sci. Instr*. 91:083301. doi: 10.1063/5.0010968

Magana Vsevolodovna, R., Santopinto, E., and Bijker, R. (2021). Transfer reactions between odd-odd and even-even nuclei by using IBFFM. *arXiv* arXiv:2101.05659v05651.

Matsubara, H., Takaki, M., Uesaka, T., Shimoura, S., Aoi, N., Dozono, M., et al. (2013). Spectroscopic Measurement in 9He and 12Be. *Few Body Syst*. 54, 1433–1436. doi: 10.1007/s00601-012-0586-9

Oliveira, J. R. B., Cappuzzello, F., Chamon, L. C., Pereira, D., Agodi, C., Bondì, M., et al. (2013). Study of the rainbow-like pattern in the elastic scattering of 16O on 27Al at Elab. = 100 MeV. *J. Phys. G Nucl. Part Phys*. 40:105101. doi: 10.1088/0954-3899/40/10/105101

Oliveira, J. R. B., Finocchiaro, P., Agodi, C., Boztosun, I., Cappuzzello, F., De Faria, P. N., et al. (2018). New spectrometer projects for challenging particle-gamma measurements of nuclear reactions. *J. Phys. Conf. Ser*. 1056:012040. doi: 10.1088/1742-6596/1056/1/012040

Oliveira, J. R. B., Moralles, M., Flechas, D., Carbone, D., Cavallaro, M., Torresi, D., et al. (2020). First comparison of GEANT4 hadrontherapy physics model with experimental data for a NUMEN project reaction case. *Eur. Phys. J. A* 56:153. doi: 10.1140/epja/s10050-020-00152-6

Pereira, D., Linares, R., Oliveira, J. R. B., Lubian, J., Chamon, L. C., Gomes, P. R. S., et al.. (2012). Nuclear rainbow in the 16O+27AL system: the role of couplings at energies far above the barrier. *Phys. Lett. B* 710, 426–429. doi: 10.1016/j.physletb.2012.03.032

Pinna, F., Calvo, D., Campostrini, M., Capirossi, V., Delaunay, F., Fisichella, M., et al. (2020b). Evaluation of target non-uniformity and dispersion effects on energy measurement resolution in NUMEN experiment. *Phys. Scripta*. 95:094002. doi: 10.1088/1402-4896/aba779

Pinna, F., Capirossi, V., Delaunay, F., Iazzi, F., Brunasso, O., Calvo, D., et al. (2020a). Tests of a cooling system for thin targets submitted to intense ions beams for the NUMEN experiment. *Acta Phys. Pol. B* 51:665. doi: 10.5506/APhysPolB.51.655

Rifuggiato, D., Calabretta, L., Cosentino, L., and Cuttone, G. (2013). "Variety of beam production at the infn lns superconducting cyclotron," in *Proceedings of Cyclotrons 2013*. (Vancouver, BC: Canada).

Sagawa, H., and Uesaka, T. (2016). Sum rule study for double gamow-teller states. *Phys. Rev. C* 94:064325. doi: 10.1103/PhysRevC.94.064325

Santopinto, E., Garcia-Tecocoatzi, H., Magana Vsevolodovna, R. I., and Ferretti, J. (2018). Heavy-ion double-charge-exchange and its relation to neutrinoless double-beta decay. *Phys. Rev. C* 98:061601. doi: 10.1103/PhysRevC.98.061601

Sartirana, D., Calvo, D., Capirossi, V., Ferraresi, C., Iazzi, F., and Pinna, F. (2020). Target manipulation in nuclear physics experimentwith ion beams. *Adv. Serv. Indust. Robot.* 84, 533–543. doi: 10.1007/978-3-030-48989-2_57

Sauli, F. (2016). The gas electron multiplier (GEM). Operating principles and applications. *Nucl. Instr. Meth. Phys. Res. A* 805, 2–24. doi: 10.1016/j.nima.2015.07.060

Shimizu, N., Menendez, J., and Yako, K. (2018). Double gamow-teller transitions and its relation to neutrinoless decay. *Phys. Rev. Lett*. 120:142502. doi: 10.1103/PhysRevLett.120.142502

Spatafora, A., Cappuzzello, F., Carbone, D., Cavallaro, M., Lay, J.-A., Acosta, L., et al. (2019). 20Ne + 76Ge elastic and inelastic scattering at 306 MeV. *Phys. Rev. C* 100:034620. doi: 10.1103/PhysRevC.100.034620

Suhonen, J., and Civitarese, O. (2012). Review of the properties of the 0νβ-β- nuclear matrix elements. *J. Phys. G* 39:124005. doi: 10.1088/0954-3899/39/12/124005

Suhonen, J. T. (2017). Value of the axial-vector coupling strength in β and ββ decays: a review. *Front. Phys*. 5:55. doi: 10.3389/fphy.2017.00055

Takahisa, K., Ejiri, H., Akimune, H., Fujita, H., Matumiya, R., Ohta, T., et al. (2017). Double charge exchange (11B,11Li) reaction for double beta decay response. *arrive* arXiv 1703.08264.

Torresi, D., Sgouros, O., Soukeras, V., Cavallaro, M., Cappuzzello, F., Carbone, D., et al. (2021). An upgraded focal plane detector for the MAGNEX spectrometer. *Nucl. Instr. Method A* 989:164918. doi: 10.1016/j.nima.2020.164918

Tudisco, S., La Via, F., Agodi, C., Altana, C., Borghi, G., Boscardin, M., et al. (2018). SiCILIA—silicon carbide detectors for intense luminosity investigations and applications. *Sensors* 18:2289. doi: 10.3390/s18072289

Vergados, J. D., Ejiri, H., and Simkovic, F. (2012). Theory of neutrinoless double-beta decay. *Rep. Prog. Phys*. 75:106301. doi: 10.1088/0034-4885/75/10/106301

Vlachoudis, V. (2009). "A Powerful But User Friendly Graphical Interface For FLUKA," in *Proceeding International Conference on Mathematics, Computational Methods and Reactor Physics, Saratoga.* (New York, NY: Springs)

Conflict of Interest: The authors declare that the research was conducted in the absence of any commercial or financial relationships that could be construed as a potential conflict of interest.